

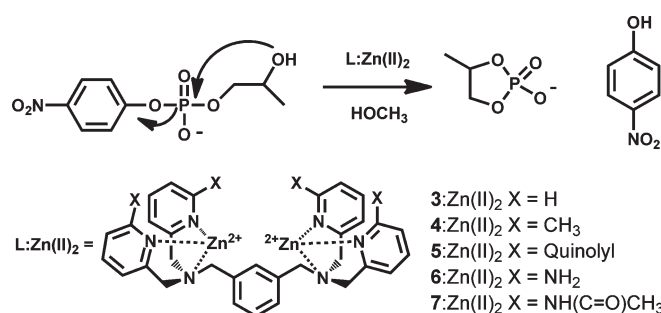
Cleavage of an RNA Model Catalyzed by Dinuclear Zn(II) Complexes Containing Rate-Accelerating Pendants. Comparison of the Catalytic Benefits of H-Bonding and Hydrophobic Substituents

Mark F. Mohamed and R. Stan Brown*

Department of Chemistry, Queen's University, Kingston, Ontario, Canada K7L 3N6

rsbrown@chem.queensu.ca

Received September 7, 2010



The transesterification of a simple RNA model, 2-hydroxypropyl *p*-nitrophenyl phosphate (**2**, HpNPP) promoted by seven dinuclear Zn(II) catalysts (**3,4,5,6,7,8,9:** $Zn(II)_2:(-OCH_3)$) based on the bis[bis(2-substituted-pyridinyl-6-methyl)]amine ligand system was investigated in methanol under s_pH -controlled conditions at 25.0 ± 0.1 °C. The two metal complexing ligands were joined together via the amino N connected to a *m*-xylyl linker (**3, 4, 5, 6, 7**) where the 2-pyridinyl substituent = H, CH₃, (CH)₄, NH₂, and NH(C=O)CH₃, respectively, and a propyl linker (**8, 9**) where the ring substituent = H and CH₃. All of the dinuclear complexes except **8:** $Zn(II)_2$ exhibit saturation kinetics for the k_{obs} versus [catalyst] plots from which one can determine catalyst:substrate binding constants (K_M), the catalytic rate constants for their decomposition (k_{cat}), and the second order catalytic rate constants ($k_2^{cat} = k_{cat}/K_M$). In the case of **8:** $Zn(II)_2$, the plots of k_{obs} versus [catalyst] as a function of s_pH are linear, and the catalytic rate constants (k_2^{cat}) are defined as the gradients of the plots. Analysis of all of the data at the s_pH optimum for each reaction indicates that the presence of the amino and acetamido H-bonding groups and the CH₃ group provides similar increases of the k_{cat} terms of 25–50 times that exhibited by the parent complex **3:** $Zn(II)_2$. However, in terms of substrate catalyst binding (K_M), there is no clear trend that H-bonding groups or the CH₃ group provides stronger binding than the parent complex. In terms of the overall second order catalytic rate constant, the CH₃, amino, and NH(C=O)CH₃ groups provide 20, 10, and 68 times the k_2^{cat} observed for the parent complex. In the case of **9:** $Zn(II)_2$, the presence of the methyl groups provides a 1000-fold increase in activity (judged by k_2^{cat}) over the parent complex **8:** $Zn(II)_2$. The results are interpreted to indicate that H-bonding effects may be important for catalysis and less so for substrate binding, but the steric effect and impact on the local polarity provided by a methyl substituent is just as effective and in fact may form part of the acceleratory effect attributed to H-bonding in related systems.

Introduction

The phosphodiester linkage is highly stable toward solvolytic cleavage and is widely utilized throughout Nature as the linker joining the backbone components of DNA and RNA polymers. Many of the enzymes that promote the cleavage of phosphate diester linkages contain two or more metal ions

(notably Zn(II) but in some cases Ca(II), Mg(II), Fe(III), and Mn(II)) in their active sites, acting cooperatively to give rate enhancements for P–O cleavage up to 10^{17} .¹ Inspired by the rate accelerations achieved by metal ion containing

(1) Schroeder, G. K.; Lad, C.; Wyman, P.; Williams, N. H.; Wolfenden, R. *Proc. Natl. Acad. Sci. U.S.A.* **2006**, *103*, 4052.

phosphodiesterases, considerable interest has developed in the design of small molecule mono- and dinuclear metal complexes that catalyze the cleavage of phosphate diesters.²

The catalytic role of the metal ions in the enzymes is thought to be enhanced by contributions from strategically located amino acid residues in the active site. The micro-environment surrounding a metal ion has been shown to play a major role in biologically relevant metal-promoted reactions.³ A recent trend in the design of metal complexes that catalyze the cleavage of phosphate esters is the incorporation of ancillary hydrogen-bonding (H-bonding) substituents that are postulated to enhance catalysis through favorable interactions with the transforming substrate in the transition state.⁴ A number of these catalysts employ ligands based on the bis(2-amino-pyridinyl-6-methyl)amine moiety that incorporates a primary amino group at the 2-position of both pyridyl rings. The observation that complexes bearing H-bond donating groups are generally more active than the corresponding unsubstituted complexes is taken as evidence that catalyst activity can be modulated by strategically incorporating the H-bonding functionality.

Recent work from this laboratory has focused on the cleavage of simple RNA and DNA models catalyzed by dinuclear Zn(II) complexes in the light alcohols methanol and ethanol.⁵ We have demonstrated that the cleavage of phosphate diesters as RNA and DNA models is accelerated by 10^{11-17} relative to the background reactions in the presence of the a system comprising an alcohol medium and the dinuclear complex **1**:Zn(II)₂.⁶⁻⁸ This system far outperforms any reported synthetic nuclease models that operate in water

and leads us to conclude that the large rate enhancements observed upon moving from aqueous solution⁹ into alcohols of lower dielectric constant and polarity stem from an important medium effect that has, until recently, been underappreciated. The importance of nonpolar surroundings has been recently demonstrated by Wolfenden,¹⁰ who reported that the spontaneous hydrolysis of a nonactivated phosphate diester mono-anion is accelerated by nearly a million times by moving from pure water to wet cyclohexane. In our hands, the alcohol medium seems to simplify, in some respects, problems encountered in water where active dinuclear M(II)₂ complexes cannot be formed unless an auxiliary oxo-bridging group is present, probably to insulate the charge repulsion between the two metal centers, thus stabilizing the dinuclear core.¹¹ The lower polarities of methanol and ethanol seem to enhance the metal binding to the ligands relative to water, probably by decreasing the solvation of the metal ions. This allows us to make highly active dinuclear Zn(II) complexes operating in alcohol without auxiliary bridging oxo groups that, when present in comparison systems, are detrimental to catalytic activity.¹²

Building on the large catalytic acceleration that results from alcohol media rather than water, we wondered if the addition of simple hydrophobic groups proximal to the dinuclear core of the catalyst might create an extended hydrophobic pocket and enhance activity through interactions similar to the hydrophobic effects observed in aqueous media.¹³ In order to test whether specifically positioned H-bonding groups might provide additional catalytic benefits in methanol, we have also prepared, for comparison with the complexes with hydrophobic substituents and for results obtained in water, complexes with a 2-NH₂ and 2-acetamido (NH(C=O)CH₃) group, both of which have been suggested to exert positive H-bonding effects on phosphate binding and cleavage in suitably substituted Zn(II) complexes.^{4,14} Herein we report a kinetic study of the cyclization of the simple RNA analogue 2-hydroxypropyl-*p*-nitrophenyl phosphate (**2**, HpNPP) in methanol catalyzed by a series of Zn(II)₂ complexes with alkyl substituents **4**:Zn(II)₂, **5**:Zn(II)₂, and **9**:Zn(II)₂, comparing their activities with the nonfunctionalized parent complexes substituted only with H, **3**:Zn(II)₂ and **8**:Zn(II)₂. The studies show that the rate of the catalyzed cleavage of **2** can be enhanced by up to 3 orders of magnitude by modification of a Zn(II)₂ catalyst with simple alkyl/alkenyl substituents (CH₃, (CH)₄). We have also studied a pair of dinuclear catalysts that are functionalized with H-bonding groups, **6**:Zn(II)₂ and **7**:Zn(II)₂. The data indicate that both H-bond donating substituents and alkyl substituents enhance catalysis relative to the unsubstituted complex, but surprisingly, the H-bond donating substituents are no

(2) For a representative list of references on various metal-containing complexes, see: (a) Mancin, F.; Tecilla, P. *New J. Chem.* **2007**, *31*, 800. (b) Weston, J. *Chem. Rev.* **2005**, *105*, 2151. (c) Molenveld, P.; Engbertsen, J. F. J.; Reinhoudt, D. N. *Chem. Soc. Rev.* **2000**, *29*, 75. (d) Williams, N. H.; Takasaki, B.; Wall, M.; Chin, J. *Acc. Chem. Res.* **1999**, *32*, 485. (e) Mancin, F.; Scrimin, P.; Tecilla, P.; Tonellato, U. *Chem. Commun.* **2005**, 2540. (f) Morrow, J. R.; Iranzo, O. *Curr. Opin. Chem. Biol.* **2004**, *8*, 192.

(3) (a) Borovik, A. S. *Acc. Chem. Res.* **2005**, *38*, 54. (b) Marque Rivas, J. C. *Curr. Org. Chem.* **2007**, *11*, 1434.

(4) For a representative example of studies on small molecule enzyme mimics utilizing hydrogen bond donors, see: (a) Feng, G.; Natale, D.; Prabakaran, R.; Marque-Rivas, J. C.; Williams, N. H. *Angew. Chem., Int. Ed.* **2006**, *45*, 7056. (b) Feng, G.; Marque-Rivas, J. C.; Williams, N. H. *Chem. Commun.* **2006**, 1845. (c) Ait-Haddou, H.; Sumaoka, J.; Wiskur, S. L.; Folmer-Anderson, J. F.; Anslyn, E. V. *Angew. Chem., Int. Ed.* **2002**, *41*, 4014. (d) Livieri, M.; Mancin, F.; Tonellato, U.; Chin, J. *Chem. Commun.* **2004**, 2862. (e) Feng, G.; Marque-Rivas, J. C.; Torres Martin de Rosales, R.; Williams, N. H. *J. Am. Chem. Soc.* **2005**, *127*, 13470. (f) Lombardo, V.; Bonomi, R.; Sissi, C.; Mancin, F. *Tetrahedron* **2010**, *66*, 2189. (g) Bonomi, R.; Saielli, G.; Tonellato, U.; Scrimin, P.; Mancin, F. *J. Am. Chem. Soc.* **2009**, *131*, 11278. (h) Bonomi, R.; Selvestrel, F.; Lombardo, V.; Sissi, C.; Polizzi, S.; Mancin, F.; Tonellato, U.; Scrimin, P. *J. Am. Chem. Soc.* **2008**, *130*, 15744. (i) Livieri, M.; Mancin, F.; Saielli, G.; Chin, J.; Tonellato, U. *Chem.—Eur. J.* **2007**, *13*, 2246.

(5) Brown, R. S. Biomimetic and non-biological dinuclear M²⁺-complex catalyzed alcoholysis reactions of phosphoryl transfer reactions. In *Progress in Inorganic Chemistry*; Karlin, K. D., Ed.; John Wiley and Sons: Hoboken, NJ, Vol. 57, in press.

(6) Neverov, A. A.; Lu, Z.-L.; Maxwell, C. I.; Mohamed, M. F.; White, C. J.; Tsang, J. S. W.; Brown, R. S. *J. Am. Chem. Soc.* **2006**, *128*, 16398.

(7) Bunn, S. E.; Liu, C. T.; Lu, Z.-L.; Neverov, A. A.; Brown, R. S. *J. Am. Chem. Soc.* **2007**, *129*, 16238.

(8) Liu, C. T.; Neverov, A. A.; Brown, R. S. *J. Am. Chem. Soc.* **2008**, *130*, 16711.

(9) Kim and Lim (Kim, J.; Lim, H. *Bull. Korean Chem. Soc.* **1999**, *20*, 491) have reported that complex **1**:Zn(II)₂ is no more reactive in water than its mononuclear analogue, the Zn(II) complex of 1,5,9-triazacyclododecane for the cleavage of bis-*p*-nitrophenyl phosphate.

(10) (a) Stockbridge, R. B.; Wolfenden, R. *Chem. Commun.* **2010**, 46, 4306. (b) See also: Stockbridge, R. B.; Wolfenden, R. *J. Am. Chem. Soc.* **2009**, *131*, 18248.

(11) Morrow, J. R. *Comments Inorg. Chem.* **2008**, *29*, 169.

(12) Mohamed, M. F.; Neverov, A. A.; Brown, R. S. *Inorg. Chem.* **2009**, *48*, 11425.

(13) (a) Blokzijl, W.; Engberts, J. B. F. N. *Angew. Chem., Int. Ed. Engl.* **1993**, *32*, 1545. (b) Otto, S.; Engberts, J. B. F. N. *Org. Biomol. Chem.* **2003**, *1*, 2809.

(14) Lee, J. H.; Park, J.; Lah, M. S.; Chin, J.; Hong, J.-I. *Org. Lett.* **2007**, *9*, 3729.

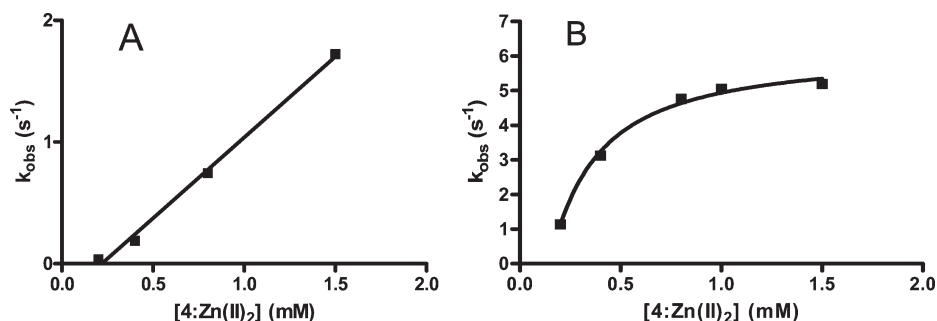
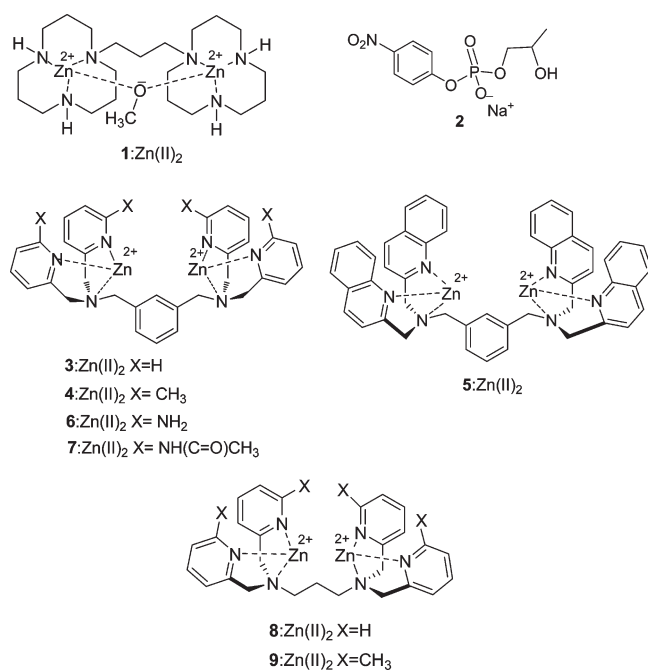


FIGURE 1. Plots of k_{obs} versus $[4:\text{Zn}(\text{II})_2]$ for the cleavage of HPNPP (**2**) (5×10^{-5} M) showing: (A) a linear dependence at $s\text{pH} = 6.90$ ($k_2^{\text{cat}} = 1327 \text{ M}^{-1} \text{ s}^{-1}$) and (B) saturation kinetics at $s\text{pH} = 7.95$ ($k_{\text{cat}} = 6.2 \text{ s}^{-1}$, $K_M = 0.21 \text{ mM}$, $k_{\text{cat}}/K_M = k_2^{\text{cat}} = 29,848 \text{ M}^{-1} \text{ s}^{-1}$) determined from the rate of appearance of 4-nitrophenol at 320 nm, $T = 25.0 \pm 0.1$ °C. Data are corrected for the effect of buffer.

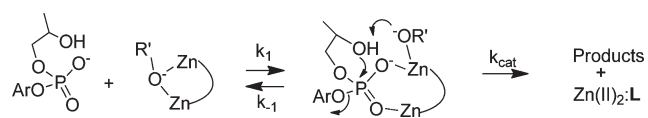
better than alkyl substituents in accelerating the cyclization of **2** in methanol.



Results

The catalyzed cleavage of **2** was studied in buffered methanol with all catalyst complexes except **7:Zn(II)₂**, and in all cases the kinetic data were corrected for buffer effects as described in the Experimental Section and Supporting Information. Kinetic experiments with **7:Zn(II)₂** were conducted in the absence of buffer due to its strong inhibition. The catalyst was formed *in situ* through sequential addition of stock solutions of sodium methoxide, ligand, and $\text{Zn}(\text{OTf})_2$ to anhydrous methanol such that $[\text{OCH}_3]:[\text{7}]:[\text{Zn}(\text{OTf})_2] = 1:1:2$. Formulation of the catalyst in this way is assumed to generate a $[\text{catalyst}] = [\text{ligand}] = 1/2[\text{Zn}(\text{II})]_{\text{total}}$ and experimentally gave solutions with $s\text{pH}$ in the range of 9.9 ± 0.4 . The data for **7:Zn(II)₂** were corrected for the effect of the triflate counterion by plotting k_{obs} for the cleavage of **2** at constant $[7:\text{Zn}(\text{II})_2]$ versus increasing [tetrabutylammonium triflate]. The inhibition data were analyzed (see Supporting Information, eq 2S) to give a triflate inhibition constant of 5.8 mM.

SCHEME 1. Proposed Pathway for the Cleavage of **2** Promoted by $\text{L}:\text{Zn}(\text{II})_2$



The plots of k_{obs} versus [catalyst] for the cleavage of **2** catalyzed by **3:Zn(II)₂**–**6:Zn(II)₂** and **9:Zn(II)₂** are $s\text{pH}$ -dependent, with all catalyst complexes showing both linear behavior (Figure 1A) and saturation binding (Figure 1B), indicative of a change in the strength of binding between the catalyst complex and the substrate as a function of $s\text{pH}$. In all cases, a significant x -intercept was observed, similar to the behavior of most other dinuclear $\text{Zn}(\text{II})$ complexes in methanol we have reported,^{5–7,11} and analyzed as being consistent with dissociation of a $\text{Zn}(\text{II})$ ion from the complex at low concentration that leads to an inactive or severely less active mononuclear form. Complex **8:Zn(II)₂** exhibited linear kinetics over the $s\text{pH}$ range studied. The second-order rate constants (k_2^{cat}) were determined as the slope of the plots of k_{obs} versus [catalyst] from the linear kinetics plots.

The observation of saturation kinetics is indicative of formation of a kinetically active catalyst:substrate complex followed by one or more chemical steps leading to the spectroscopically observed product (Scheme 1). Where saturation kinetics were observed, the data were fit to the universal binding equation, eq 1,¹⁵ to obtain values of k_{cat} (the maximum observed rate constant) and K_M (the $[\text{L}:\text{Zn}(\text{II})_2]:[\text{2}]$ dissociation constant, taken as the reciprocal of the binding constant, K_B from eq 1). In these cases, the apparent second order catalytic rate constant is given as $k_{\text{cat}}/K_M = k_2^{\text{cat}}$. The variable [cat] in eq 1 refers to the total concentration of catalyst introduced into the solution, where $[\text{ligand}]:[\text{Zn}(\text{II})] = 1:2$.

$$k_{\text{obs}} = k_{\text{cat}}(1 + K_B[\text{S}] + [\text{cat}]K_B - X)/(2K_B)/[\text{S}] \quad (1)$$

where

$$X = (1 + 2K_B[\text{S}] + 2[\text{cat}]K_B + K_B^2[\text{S}]^2 - 2K_B^2[\text{cat}][\text{S}] + [\text{cat}]^2K_B^2)^{0.5}$$

The k_{obs} versus [catalyst] plot obtained with **7:Zn(II)₂** also showed curvature suggestive of the formation of a

(15) Equation 1 was obtained from the equations for equilibrium binding and for conservation of mass by using the commercially available MAPLE software: *Maple 9.00*, June 13, 2003, Build ID 13164; Maplesoft, a division of Waterloo Maple Inc.: Waterloo, Ontario, Canada, 1981–2003.

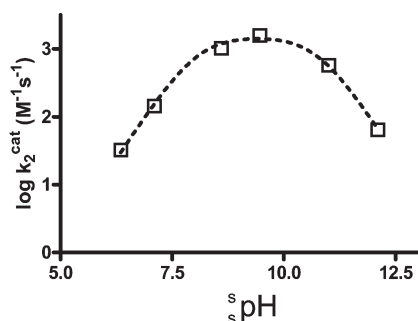
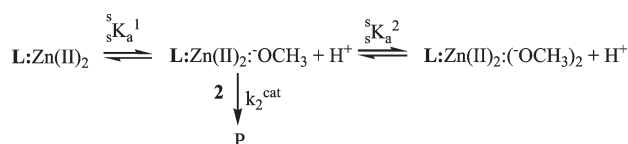


FIGURE 2. Plot of $\log k_2^{\text{cat}}$ versus ${}^s\text{pH}$ for the methanolysis of 0.05 mM **2** catalyzed by **3:Zn(II)₂**. The dashed line through the data points is calculated from the fit of the data to eq 2, which gives ${}^s\text{p}K_a^1 = 8.1 \pm 0.1$, ${}^s\text{p}K_a^2 = 10.8 \pm 0.1$, and $k_2^{\text{max}} = (1.5 \pm 0.2) \times 10^3 \text{ M}^{-1} \text{ s}^{-1}$.

SCHEME 2. ${}^s\text{pH}$ -Dependent Process for the Cleavage of **2** Mediated by **L:Zn(II)₂**:(-OCH₃)



catalyst–substrate complex. Values of k_{cat} and K_M were determined by fitting the corrected kinetic data to eq 1.

The $\log k_2^{\text{cat}}$ versus ${}^s\text{pH}$ plots for all catalysts is bell-shaped (see Supporting Information and representative plot in Figure 2 with **3:Zn(II)₂**), consistent with the formation of an active complex with H⁺-dissociation from the complex, followed by a second ionization leading to loss of catalysis.

The $\log k_2^{\text{cat}}$ versus ${}^s\text{pH}$ data were fit to eq 2 (derived from the kinetic process in Scheme 2) to give kinetic ${}^s\text{p}K_a$ values. In the case of **7:Zn(II)₂**, for ${}^s\text{pH}$ values below 9.5 and above 11.1, the absolute slope of the plot of $\log k_2^{\text{cat}}$ versus ${}^s\text{pH}$ is much greater than unity, which we interpret as being due to an instability of the catalyst complex outside this ${}^s\text{pH}$ range. The data outside this ${}^s\text{pH}$ range were omitted from the nonlinear fit (for a more detailed discussion of the treatment of the ${}^s\text{pH}$ -rate data for **7:Zn(II)₂** see Supporting Information).

$$k_2^{\text{cat}} = \left(\frac{k_2^{\text{max}} \cdot {}^sK_a^1 \cdot [\text{H}^+]}{[\text{H}^+]^2 + [\text{H}^+] \cdot {}^sK_a^1 + {}^sK_a^1 \cdot {}^sK_a^2} \right) \quad (2)$$

The various kinetic parameters (k_{cat} , K_M , and $k_{\text{cat}}/K_M = k_2^{\text{cat}}$) and ${}^s\text{p}K_a$ values for each catalyst operating at its optimal ${}^s\text{pH}$ (defined as the ${}^s\text{pH}$ where the maximum catalytic rate for each complex is observed) are summarized in Table 1. With the exception of **8:Zn(II)₂**, for which all plots of k_{obs} versus ${}^s\text{pH}$ were linear, the change in the shape of the plot of k_{obs} versus ${}^s\text{pH}$ from linear to curved as a function of ${}^s\text{pH}$ suggests an increasing tightness of binding of the substrate and complex up to the ${}^s\text{pH}$ -rate maximum, above which the K_M value steadily increases (binding becomes weaker). In the case of **5:Zn(II)₂**, binding of the substrate to the catalyst complex was only observed at the ${}^s\text{pH}$ -rate maximum (${}^s\text{pH} = 8.50$), whereas plots of k_{obs} versus ${}^s\text{pH}$ were linear at all other ${}^s\text{pH}$ values. Since the active form of the catalysts is thought to be the monomethoxy form,

we believe that the increase in the tightness of binding upon approaching the ${}^s\text{pH}$ -rate maximum is attributed to the introduction of a transient methoxide bridge between the two Zn(II) ions that preorganizes them into a configuration that is optimal for binding the anionic substrate in a bidentate fashion. The introduction of a second methoxide at higher ${}^s\text{pH}$ has the dual effect of neutralizing the positive charge of the Zn(II) centers and possibly disrupting the configuration of the catalyst, which weakens the binding between the catalyst and substrate.

Discussion

The bis(2-pyridylmethyl)amine scaffold is useful for this study because of its well-demonstrated use in various Zn(II) catalysts^{4,17} and the easy access to substituted derivatives.¹⁸ It also serves as an appropriate comparison of the results herein with those from past work since the bis(2-amino-pyridinyl-6-methyl)amine unit has been commonly used for the study of the effects of H-bonding pendants on the phosphate binding characteristics and catalysis of cleavage of phosphate substrates.^{4,14}

1. Cleavage of **2 Catalyzed by Complexes **3:Zn(II)₂** to **7:Zn(II)₂**.** It is a striking feature of the data in Table 1 that all of the functionalized catalyst complexes (**4**, **5**, **6**, **7**, where X = CH₃, (CH)₄, NH₂, and NH(C=O)CH₃) respectively) exhibit a greater activity than the parent complex (**3:Zn(II)₂**, where X = H). Since all of the Zn(II)₂ complexes of **3–7** exhibit saturation kinetics, a direct comparison of the effect of substituent can be made for both substrate binding (K_M) and catalytic rate constant (k_{cat}) for substrate cleavage within the **L:Zn(II)₂:**2**** complex. All **L:Zn(II)₂** systems show comparable affinity for substrate as judged by the K_M values in Table 1, varying by at most a factor of ~ 10 (7.3×10^{-4} M for **5:Zn(II)₂** and 6.6×10^{-5} M for **7:Zn(II)₂**). While it is tempting to suggest that the H-bonding possible in **7:Zn(II)₂**¹⁴ will lead to tighter substrate binding by this complex, its K_M is comparable to that of the parent complex **3:Zn(II)₂** (7.8×10^{-5} M), suggesting that the putative H-bonding is not beneficial to stabilizing the Michaelis complex. Direct comparison of the K_M values of **4:Zn(II)₂** (X = CH₃) and **6:Zn(II)₂** (X = NH₂) indicates these are essentially the same, 2.1×10^{-4} and 2.4×10^{-4} M, respectively, indicating that the possible H-bonding amino group provides the same net effect that the non-H-bonding methyl group does. In fact, considering that the K_M value is the dissociation constant for the **L:Zn(II)₂:(-OCH₃)₂** complex or its kinetic equivalent, **L:Zn(II)₂:⁻** (where the 2-hydroxypropyl group of the bound substrate is deprotonated by the internal methoxide),¹⁹ both of these complexes bind substrate slightly weaker (about 3 times) than does the parent **3:Zn(II)₂**. The relative invariance of binding between the dinuclear complexes and diester **2** is surprising but consistent with the recent findings of Gunning et al.,¹⁸ who found no

(16) The computed values of ${}^s\text{p}K_a^1$ and ${}^s\text{p}K_a^2$ for **4:Zn(II)₂** are very similar and heavily correlated to each other and with k_2^{cat} . This precludes an exact numerical determination of these parameters. The values listed in Table 1 are the lower and upper limits for ${}^s\text{p}K_a^1$ and ${}^s\text{p}K_a^2$, respectively.

(17) Yashiro, M.; Kaneiwa, H.; Onaka, K.; Komiyama, M. *Dalton Trans.* **2004**, 605.

(18) Drewry, J. A.; Fletcher, S.; Hassan, H.; Gunning, P. T. *Org. Biomol. Chem.* **2009**, *7*, 5074.

(19) (a) Yang, M.-Y.; Iranzo, O.; Richard, J. P.; Morrow, J. R. *J. Am. Chem. Soc.* **2005**, *127*, 1064. (b) Feng, G.; Mareque-Rivas, J. C.; Torres Martn de Rosales, R.; Williams, N. H. *J. Am. Chem. Soc.* **2005**, *127*, 13470.

TABLE 1. Kinetic Constants (k_{cat} , K_{M} , and $k_{\text{cat}}/K_{\text{M}} = k_2^{\text{cat}}$) and Kinetic $\text{s}^{\text{p}}K_{\text{a}}$ Values for the Cleavage of **2** (0.05 mM) Catalyzed by the L:Zn(II)₂ Complexes of Ligands **3–9** under Optimal $\text{s}^{\text{p}}\text{H}$ Conditions^a in Methanol at $T = 25.0 \pm 0.1$ °C

| complex | $\text{s}^{\text{p}}K_{\text{a}}^1$ | $\text{s}^{\text{p}}K_{\text{a}}^2$ | k_{cat} (s ⁻¹) | K_{M} (M) | $k_{\text{cat}}/K_{\text{M}} = k_2^{\text{cat}}$ (M ⁻¹ s ⁻¹) |
|-------------------------------|-------------------------------------|-------------------------------------|-------------------------------------|--------------------------------|-------------------------------------------------------------------------------------|
| 3 :Zn(II) ₂ | 8.1 ± 0.1 | 10.8 ± 0.1 | 0.13 ± 0.01 | (7.8 ± 3.5) × 10 ⁻⁵ | (1.6 ± 0.7) × 10 ³ |
| 4 :Zn(II) ₂ | ≥ 8.4 ^b | ≤ 8.3 ^b | 6.2 ± 0.4 | (2.1 ± 0.5) × 10 ⁻⁴ | (29.8 ± 7.0) × 10 ³ |
| 5 :Zn(II) ₂ | 8.9 ± 0.4 | 8.5 ± 0.4 | 4.3 ± 0.8 | (7.3 ± 3.2) × 10 ⁻⁴ | (5.9 ± 2.7) × 10 ³ |
| 6 :Zn(II) ₂ | 7.7 ± 0.5 | 10.2 ± 0.5 | 3.89 ± 0.03 | (2.4 ± 0.1) × 10 ⁻⁴ | (16 ± 1) × 10 ³ |
| 7 :Zn(II) ₂ | 9.7 ± 0.5 | 10.1 ± 0.4 | 7.2 ± 0.3 | (6.6 ± 0.9) × 10 ⁻⁵ | (109 ± 5) × 10 ³ |
| 8 :Zn(II) ₂ | 9.6 ± 0.3 | 10.8 ± 0.3 | NA | NA | (31 ± 1) ^c |
| 9 :Zn(II) ₂ | 9.0 ± 0.7 | 9.9 ± 0.7 | 3.2 ± 0.1 | (9.4 ± 2.2) × 10 ⁻⁵ | (34.0 ± 8.0) × 10 ³ |

^aOptimal $\text{s}^{\text{p}}\text{H}$ defined as highest experimental value for k_{cat} in the $\text{s}^{\text{p}}\text{H}$ /rate constant profile. ^bSee ref 16. ^cThe second-order rate constants are determined from the slope of the linear plot of k_{obs} versus [L:Zn(II)₂]

remarkable differences in the binding constant between a series of phosphate esters and **3**:Zn(II)₂, **6**:Zn(II)₂, and **7**:Zn(II)₂ as determined by isothermal titration calorimetry. The values of K_{M} reported in Table 1 refer to the binding constants determined from fitting of the data to eq 1 at the optimal $\text{s}^{\text{p}}\text{H}$ for each catalyst complex under the assumption that all of the catalyst is capable of binding the substrate ([cat] = [ligand] = 1/2[Zn(II)]). However, at the $\text{s}^{\text{p}}\text{H}$ values obtained at the maxima of the various $\text{s}^{\text{p}}\text{H}$ -rate profiles, the concentration of the active monomethoxy species (Scheme 2) is less than the total concentration of catalyst complex in solution (particularly so in the cases where $\text{s}^{\text{p}}K_{\text{a}}^1$ and $\text{s}^{\text{p}}K_{\text{a}}^2$ are similar, as in **4**:Zn(II)₂ and **5**:Zn(II)₂). Given this consideration, the values of K_{M} in Table 1 may be considered as upper limits.²⁰ This effect may also contribute to the absence of a clear trend in K_{M} values but does not alter the interpretation of the k_{cat} values.

At first glance, the kinetic parameters listed in Table 1 suggest that **5**:Zn(II)₂ is the least active of the catalysts, with a k_2^{cat} of only $5.9 \times 10^3 \text{ M}^{-1} \text{ s}^{-1}$ compared to $109 \times 10^3 \text{ M}^{-1} \text{ s}^{-1}$ for **7**:Zn(II)₂. Inspection of the kinetic constants reveals that **5**:Zn(II)₂ has a k_{cat} value slightly less than that of **7**:Zn(II)₂ and comparable to that of **6**:Zn(II)₂. The difference in second-order rate constants arises from weaker binding of the substrate by **5**:Zn(II)₂, over 10-fold weaker than the binding between the substrate and **7**:Zn(II)₂, which may be attributable to steric crowding. The fact that the k_{cat} term for **5**:Zn(II)₂ is comparable to those of **4**:Zn(II)₂, **6**:Zn(II)₂, and **7**:Zn(II)₂ indicates that, once bound to the substrate, it will catalyze the latter's conversion to products at the same rate as the other functionalized catalysts.

The major difference between the bis(2-substituted pyridinyl-6-methyl)amino complexes and the parent complexes studied here is in the k_{cat} terms given in Table 1. In all cases, the substituted complexes have k_{cat} terms greater than the parent complex by over an order of magnitude; while all of the complexes are able to bind the substrate with similar affinity, the 2-substituted complexes excel at promoting the cleavage of the bound substrate. It is interesting that the k_{cat} values for all of the substituted complexes fall within a very narrow range, suggesting that the different substituents (be they amino, acetamido or alkyl) are all equally capable of stabilizing

the transition state for the chemical cleavage step in Scheme 1 relative to what is provided by the parent complexes. It is also significant that the k_{cat} values for **6**:Zn(II)₂ and **7**:Zn(II)₂ differ by only a factor of 2 despite a large difference in the H-bond donating abilities of the NH₂ and NH(C=O)CH₃ groups. The Taft–Kamlet α -parameters (a measure of a protic solvent's hydrogen bond donating ability)²¹ for aniline (0.26) and *N*-methylformamide (0.62)²² give a rough estimate of the H-bond donating ability of the NH₂ and NH(C=O)CH₃ substituents, suggesting that the N–H bond of the amide should be a significantly better hydrogen-bond donor than the N–H bond of an aniline type amine. It appears that the large difference in H-bond donating ability is subtly manifested in the strength of substrate binding by **6**:Zn(II)₂ and **7**:Zn(II)₂ (K_{M} differs by ~3.5) and the catalytic rate constant (factor of 2) so that the overall difference in the $k_{\text{cat}}/K_{\text{M}}$ terms is at most 7-fold for these two complexes. Furthermore the fact that the ordering of k_{cat} (and K_{M}) for **4**:Zn(II)₂ (where the CH₃ substituent is expected to have $\alpha = 0^{27}$), **6**:Zn(II)₂, and **7**:Zn(II)₂ is 6.2, 3.9, and 7.2 s⁻¹, respectively (30×10^{-3} , 16×10^{-3} and $109 \times 10^{-3} \text{ M}^{-1} \text{ s}^{-1}$, respectively), is evidence that H-bonding cannot be said to be significantly more effective than whatever is responsible for the CH₃ groups' effect is in improving catalysis relative to the parent, **3**:Zn(II)₂.

2. Cleavage of 2 Catalyzed by 8:Zn(II)₂ and 9:Zn(II)₂. To give further evidence for the acceleratory properties of simple CH₃ substituents and to confirm that the catalysis observed with **4**:Zn(II)₂ is not unique for the xylyl structures, we investigated **8**:Zn(II)₂ and **9**:Zn(II)₂, where the two Zn(II)-complexing ligands are connected by a flexible propyl linker. The k_{obs} values for the cleavage of **2** promoted by **9**:Zn(II)₂ are much greater than those for **8**:Zn(II)₂ over the same concentration range (see Supporting Information). Because the k_{obs} versus [**8**:Zn(II)₂] plots are strictly linear, we can obtain only a second order rate constant for the catalyzed reaction of $k_2^{\text{cat}} = 31 \text{ M}^{-1} \text{ s}^{-1}$ from the slope of the plots. However, the k_{obs} versus [**9**:Zn(II)₂] plots show evidence of saturation binding, so it is possible to obtain both the k_{cat} and K_{M} terms as well as a k_2^{cat} of $34 \times 10^3 \text{ M}^{-1} \text{ s}^{-1}$ indicating that **9**:Zn(II)₂ is ~10³ more reactive than **8**:Zn(II)₂. The presence of the CH₃ groups in **9**:Zn(II)₂ affords stronger substrate binding relative to **8**:Zn(II)₂, comparable to what is seen in the best of the xylyl cases, as well as a k_{cat} term that is similar to what is seen for the xylyl complexes where X = alkyl, NH₂, or NH(C=O)CH₃.

(20) Computation of the amounts of the neutral, monomethoxy, and dimethoxy forms of the catalyst (Scheme 2) from the various $\text{s}^{\text{p}}K_{\text{a}}^1$ and $\text{s}^{\text{p}}K_{\text{a}}^2$ values indicates that the amount of monomethoxy plus neutral forms of the catalyst (the ones most likely to bind the anionic substrate) range from 95% (for **3**:Zn(II)₂) to 62% (for **7**:Zn(II)₂). Under the assumption that these two forms are the ones responsible for substrate binding, the actual K_{M} values would be 95–71% less than those in Table 1. However, the uncertainties in the various K_{M} and $\text{s}^{\text{p}}K_{\text{a}}$ values computed from fits of the experimental data to eq 2 indicate that these kinds of corrections to the K_{M} values in Table 1 are unwarranted.

(21) (a) Taft, R. W.; Kamlet, M. J. *J. Am. Chem. Soc.* **1976**, *98*, 2886.

(b) Kamlet, M. J.; Abboud, J.-L. M.; Abraham, M. H.; Taft, R. W. *J. Org. Chem.* **1983**, *48*, 2877.

(22) Marcus, Y. *J. Solution Chem.* **1991**, *20*, 929.

Conclusions

The above findings point out that caution should be exercised in rationalizing the accelerating effect of H-bond donating substituents on complexes cleaving phosphate diesters such as **2**. Where such arguments are made, they are largely based on enhanced reaction rate compared to a complex without the H-bonding group and X-ray diffraction evidence on bound substrates or surrogates.^{4a,14} However, the latter structural evidence only confirms the possibility of H-bonding interactions in the ground state but does not require that these interactions are maintained (and necessarily strengthened) in the transition state for the chemical reaction. Even so, an observed accelerating effect designated to a suitably placed H-bonding group may be difficult to ascribe unambiguously without a more extensive set of comparisons.

We have shown that the cleavage of a phosphate diester **2** catalyzed by several Zn(II)₂ complexes based on the bis[bis-(2-X-, 6-pyridylmethyl)amino] propyl and xylyl systems is accelerated by at least two and perhaps more effects resulting from functionalization of the catalyst with X = CH₃, NH₂, NH(C=O)CH₃, and (CH)₄ groups. Functionalization of the catalyst with hydrophobic and sterically demanding CH₃ groups seems to be an effective strategy to enhance catalysis without invoking any H-bonding effects. The activities of the CH₃-substituted systems is comparable to the effects afforded by NH₂ and NH(C=O)CH₃ substituents. While the importance of H-bonding interactions in enzymatic reactions is well established,^{3,23} the ability to mimic them with simple model systems has been less conclusively demonstrated, particularly since other effects such as steric, local polarity, and medium-induced ones now seem to be as important in such systems as are presented here. Given that the 2-NH₂ group and 2-CH₃ groups are roughly iso-structural with similar steric demands, it is difficult to decide which of H-bonding or steric effects is the more important. While we cannot unambiguously rule out H-bonding as a mode of activation, our findings suggest that the acceleratory effects of H-bond donating substituents may be the result of a general, and perhaps more complex effect of substitution at the 2-position of the pyridyl rings of the bis[bis(2-X-, 6-pyridylmethyl)]amino metal receptors.

Experimental Section

1. Synthesis. The syntheses of bis[bis(2-pyridylmethyl)amino]-*m*-xylene (**3**)²⁴ and 1,3-bis[bis(2-pyridylmethyl)amino]propane (**8**)²⁵ were accomplished as previously reported.

Bis[bis(2-methyl 6-pyridylmethyl)amino]-*m*-xylene (4**).** To a suspension of 2-bromomethyl-6-methylpyridine²⁶ (3.6 g, 19.3 mmol) in 20 mL of water was added *m*-xylylenediamine (0.54 mL, 0.57 g, 4.2 mmol) followed by solid NaOH (2.0 g, 50.0 mmol). The dark red mixture was stirred vigorously and heated to reflux for 24 h. The aqueous mixture was cooled to room temperature, 50 mL of CHCl₃ was added, and the layers were separated. The aqueous phase was extracted with an additional 50 mL of CHCl₃. The combined organic layers were washed once with

50 mL of saturated brine and dried over Na₂SO₄. Evaporation of the solvent gave a dark brown viscous oil that was suspended in 50 mL of hexanes to immediately precipitate a brown powder that was removed by filtration. The filtrate was evaporated to yield an orange oil, which was taken up in a minimum amount of hot hexanes. Cooling of this solution in an ice bath caused a sticky orange residue to deposit on the walls of the flask, leaving behind a golden yellow solution. The yellow solution was decanted and placed in the freezer. After several hours, a white powder precipitated that was collected by vacuum filtration. Yield: 1.0 g (43%). Mp = 59–61 °C. ¹H NMR (300 MHz, CDCl₃): δ 2.49 (s, 12H), 3.69 (s, 4H), 3.80 (s, 8H), 6.97 (d, 4H, *J* = 9 Hz), 7.27 (m, 3H), 7.41–7.52 (m, 9H). ¹³C NMR (300 MHz, CDCl₃): δ 24.3, 58.4, 59.9, 119.5, 121.5, 127.6, 128.2, 129.2, 136.8, 138.8, 157.4, 158.8. HRMS (EI-TOF) calcd for C₃₆H₄₀N₆ (M⁺): 556.3314; found 556.3328. Anal. Calcd for C₃₆H₄₀N₆: C, 77.64; H, 7.24; N, 15.10. Found: C, 77.52; H, 7.32; N, 15.21.

Bis[bis(2-quinolylmethyl)amino]-*m*-xylene (5**).** To a suspension of 2-bromomethylquinoline²⁷ (1.8 g, 8.2 mmol) in 20 mL of water was added *m*-xylylenediamine (0.23 mL, 0.24 g, 1.8 mmol) followed by solid NaOH (0.96 g, 24.0 mmol). The two-phase mixture was stirred vigorously, heated to reflux for 24 h, and then cooled to room temperature. CHCl₃ (50 mL) was added, and the layers were separated. The aqueous phase was extracted with an additional 50 mL of CHCl₃. The combined organic layers were washed once with 50 mL of saturated brine and dried over Na₂SO₄. Evaporation of the solvent gave a dark orange viscous oil, which was purified by flash silica gel chromatography using a Biotage SP1 purification system eluting with 10:0.75 CHCl₃/HOCH₃. The fractions containing the product were combined, and the solvent was evaporated to give a viscous orange oil, which was taken up in a minimum amount of hot hexanes. Upon cooling in an ice bath, a sticky orange residue separated from a golden yellow solution. The solution was decanted and placed in the freezer overnight during which an off-white powder precipitated that was collected by filtration. Yield: 0.6 (48%). Mp = 73–76 °C. ¹H NMR (300 MHz, CDCl₃): δ 3.75 (s, 4H), 4.02 (s, 8H), 7.29 (m, 2H), 7.46 (t, 4H, *J* = 6 Hz), 7.58–7.75 (m, 14H), 8.0 (dd, 8H, *J* = 9 Hz, 21 Hz). ¹³C NMR (300 MHz, CDCl₃): δ 59.0, 61.1, 121.1, 126.3, 127.5, 127.6, 128.2, 128.4, 129.2, 129.6, 129.8, 136.5, 139.2, 147.7, 160.6. HRMS (ESI-TOF) calcd for C₄₈H₄₁N₆ (M-H⁺): 701.3392; found 701.3364. Anal. Calcd for C₄₈H₄₀N₆: C, 82.26; H, 5.75; N, 11.99. Found: C, 82.57; H, 5.60; N, 11.93.²⁸

Bis[bis(2-amino 6-pyridylmethyl)amino]-*m*-xylene (6**).** To a mixture of 2-pivaloylamino-6-bromomethylpyridine²⁹ (2.07 g, 7.6 mmol) and K₂CO₃ (0.68 g, 4.9 mmol) in 50 mL of anhydrous acetonitrile was added *m*-xylylenediamine (0.247 mL, 0.26 g, 1.91 mmol). The stirring mixture was heated to reflux under N₂ atmosphere overnight. The reaction mixture was cooled to room temperature and filtered to remove the insoluble inorganic salts, which were washed with an additional 10 mL of acetonitrile. The filtrate was evaporated to yield bis[bis(2-pivaloylamino 6-pyridylmethyl)amino]-*m*-xylene as an orange foam (1.66 g, 97%), which was carried on to the next step without further purification. ¹H NMR (300 MHz, CD₃OD): δ 1.30 (s, 36H), 3.70 (s, 12H), 7.30 (m, 7H), 7.48 (s, 1H), 7.70 (t, 4H, *J* = 6 Hz), 7.96 (d, 4H, *J* = 6 Hz). ¹³C NMR (400 MHz, CD₃OD): δ 23.2, 27.6,

(27) Zhao, Q.; Liu, S.; Li, Y.; Wang, Q. *J. Agric. Food Chem.* **2009**, *57*, 2849.

(28) Elemental analysis measurements were obtained using a Thermo Scientific Flash 2000 Organic Elemental Analyzer (FlashEA 1112 series). It should be noted that using this instrument we were required to analyze compound **5** several times to obtain a carbon content that was consistent with the calculated value. In combination with the elemental analysis results, the ¹H and ¹³C NMR and HRMS data are all consistent with the desired compound.

(29) Martinho, M.; Banse, F.; Sinton, J.; Philouze, C.; Guillot, R.; Blain, G.; Dorlet, P.; Lecomte, S.; Girerd, J. *J. Inorg. Chem.* **2007**, *46*, 1709.

(23) (a) Krämer, R. *Coord. Chem. Rev.* **1999**, *182*, 243. (b) Sträter, N.; Lipscomb, W. N.; Klabunde, T.; Krebs, B. *Angew. Chem., Int. Ed.* **1996**, *35*, 2024.

(24) Gultneh, Y.; Ahvazi, B.; Khan, A. R.; Butcher, R. J.; Tuchagues, J. P. *Inorg. Chem.* **1995**, *34*, 3633.

(25) Hofmann, A.; van Eldik, R. *Dalton Trans.* **2003**, 2979.

(26) Zhang, J.; Leitun, G.; Ben-David, Y.; Milstein, D. *J. Am. Chem. Soc.* **2005**, *127*, 10840.

40.8, 59.9, 60.7, 113.9, 120.1, 129.2, 129.4, 130.7, 140.0, 152.4, 159.3, 179.5. HRMS (ESI-TOF) calcd for $C_{52}H_{69}N_{10}O_4$ ($M-H^+$): 897.5503; found 897.5455.

To a solution of bis[bis(2-pivaloylamino 6-pyridylmethyl)amino]-*m*-xylene (1.66 g, 1.85 mmol) in 100 mL of ethanol was added 100 mL of 10 M aqueous NaOH. The mixture was heated to reflux overnight with vigorous stirring. The volume of the solution was reduced to ~100 mL by rotary evaporation, and the resulting mixture was diluted with an additional 50 mL of water. The aqueous mixture was extracted with 3×100 mL $CHCl_3$, and the combined organic extracts were dried over Na_2SO_4 . The solvent was evaporated under vacuum to give a yellow foam. The foam was recrystallized from THF to give a crystalline material that became a white powder upon drying. Yield: 0.8 g (77%). Mp = 150–154 °C. 1H NMR (400 MHz, CD_3OD): δ 3.52 (s, 8H), 3.62 (s, 4H), 6.41 (d, 4H, $J = 8$ Hz), 6.91 (d, 4H, $J = 8$ Hz), 7.22 (s, 2H), 7.23 (s, 1H), 7.38 (t, 3H, $J = 8$ Hz), 7.58 (s, 1H). ^{13}C NMR (400 MHz, CD_3OD): δ 59.7, 60.6, 108.3, 112.5, 128.8, 129.2, 129.9, 139.7, 140.5, 158.7, 160.5. HRMS (ESI-TOF) calcd for $C_{32}H_{37}N_{10}$ ($M-H^+$): 561.3202; found 561.3214. The spectral data match those recently reported by Gunning et al.,¹⁸ who prepared the title compound by an alternate synthetic route.

Bis[bis(2-acetyl amino 6-pyridylmethyl)amino]-*m*-xylene (7). To a mixture of 2-acetyl amino-6-bromomethylpyridine^{4d} (1.5 g, 6. mmol) and K_2CO_3 (0.6 g, 4.4 mmol) in 20 mL of anhydrous acetonitrile was added *m*-xylylenediamine (0.22 mL, 0.23 g, 1.6 mmol). The stirring mixture was heated to reflux under N_2 atmosphere overnight. The reaction mixture was cooled to room temperature and filtered to remove the insoluble inorganic salts which were washed with an additional 10 mL acetonitrile. The filtrate was evaporated to yield an orange foamy residue, which was purified by flash silica gel chromatography on a Biotage SP1 purification system using $CH_2Cl_2/HOCH_3/NH_4OH$ (10:0.75:0.1) as the eluent ($R_f = 0.18$). The yellow solid obtained after chromatography was further purified by suspension in hot diethyl ether (20 mL) followed by filtration to yield a fluffy off-white solid. Yield: 1.0 g (84%). Mp = 125–130 °C. 1H NMR (400 MHz, CD_3OD): δ 2.11 (s, 12H), 3.65 (s, 12H), 7.23–7.27 (m, 7H), 7.51 (s, 1H), 7.65 (t, 4H, $J = 8$ Hz), 7.91 (d, 4H, $J = 8$ Hz). ^{13}C NMR (400 MHz, CD_3OD): δ 23.9, 59.6, 60.6, 113.6, 119.9, 129.0, 129.2, 130.6, 136.7, 140.3, 152.4, 159.6, 172.0. HRMS (ESI-TOF) calcd for $C_{40}H_{45}N_{10}O_4$ ($M-H^+$): 729.3625; found 729.3618. The spectral data match those recently reported by Gunning et al.,¹⁸ who prepared the title compound by an alternate synthetic route.

1,3-Bis[bis(2-methyl 6-pyridylmethyl)amino]propane (9). To a suspension of 2-bromomethyl-6-methylpyridine²⁶ (5.7 g, 31.0 mmol) in 20 mL of water was added 1,3-diaminopropane (0.55 mL, 0.49 g, 6.6 mmol) followed by solid NaOH (3.2 g, 80.0 mmol). The dark red mixture was stirred vigorously and heated to reflux for 24 h. The aqueous mixture was cooled to room temperature, 50 mL of CH_2Cl_2 was added, and the layers were separated. The aqueous phase was extracted with an additional 40 mL of CH_2Cl_2 , and the combined organic layers were dried over Na_2SO_4 . Evaporation of the solvent gave a dark brown viscous oil, which was chromatographed on a silica gel column, eluting with 10:1 $CH_2Cl_2/HOCH_3$ to afford a pale orange oil. The oil was taken up in a minimum amount of hot hexanes, which upon cooling in the freezer overnight yielded a white powder that was collected by filtration. Yield: 0.54 g (17%). Mp = 78–81 °C. 1H NMR (400 MHz, $CDCl_3$): δ 1.80 (s, 2H), 2.49 (s, 12H), 2.55 (m, 4H), 3.73 (s, 8H), 6.96 (d, 4H, $J = 8$ Hz), 7.26 (d, 4H, $J = 8$ Hz), 7.47 (t, 4H, $J = 8$ Hz). ^{13}C NMR (300 MHz, $CDCl_3$): δ 25.1, 53.1, 61.2, 120.1, 121.9, 137.2, 158.0, 160.0. HRMS (EI-TOF) calcd for $C_{31}H_{38}N_6$ (M^+): 494.3158; found 494.3177.

2. Methods. Kinetics in Methanol using UV–vis Spectroscopy. The rates of catalyzed cleavage of **2** (0.05 mM) were monitored

by UV–vis spectrophotometry at 25.0 ± 0.1 °C by observing the rate of appearance of *p*-nitrophenol at 320 nm or *p*-nitrophenolate at 400 nm. All kinetic experiments were performed with catalyst formed *in situ* through sequential addition of stock solutions (typically 100–200 mM) of ligand and $Zn(OTf)_2$ to buffered methanol solutions to make a total volume of 2.5 mL in quartz cuvettes. Reactions were initiated by the addition of 25 μ L of 5 mM substrate to the catalyst solution. Buffer solutions were prepared using mixtures of amines and HOTf in methanol to adjust the s_pH^{30} of the solution (2-picoline, $s_pH = 6.20$ – 6.40 ; 2,6-lutidine, $s_pH = 6.90$ – 7.30 ; *i*-Pr-morpholine, $s_pH = 8.00$ – 9.50 ; triethylamine, $s_pH = 10.85$ – 11.25 ; 2,2,6,6-tetramethylpiperidine, $s_pH = 12.00$ – 12.10). Where buffer inhibition was observed, plots of k_{obs} versus [buffer] were linear with a downward slope. Extrapolation of the plot of k_{obs} versus [buffer] to zero concentration gave a buffer-free rate constant that was used to correct the original experimental data (see Supporting Information). The reported values of the pseudo-first-order rate constants (k_{obs}) for the production of *p*-nitrophenol(phenolate) are the averages of duplicate runs.

The kinetics of the reactions with half-life times less than ~5 s were determined using a stopped-flow reaction analyzer thermostatted at 25.0 °C. Catalyst complexes were formed *in situ* in 4-dram vials, transferred to glass syringes, and loaded onto the stopped-flow reaction analyzer. Reaction rates were determined from the rate of appearance of *p*-nitrophenol at 320 nm or *p*-nitrophenolate at 400 nm. At least four replicate experiments were performed at each catalyst concentration, and the reported values of pseudo-first-order rate constants (k_{obs}) are the averages.

The $CH_3OH_2^+$ concentrations for the various kinetic runs were determined potentiometrically using a combination glass electrode (Radiometer model no. XC100-111-120-161) calibrated with certified standard aqueous buffers (pH = 4.00 and 10.00). The measured s_wpH meter readings in methanol were converted to the s_pH values by subtracting the δ correction factor of -2.24 .³⁰

Acknowledgment. The authors gratefully acknowledge the generous support of the Natural Sciences and Engineering Research Council of Canada (NSERC), the United States Defense Threat Reduction Agency-Joint Science and Technology Office, Basic and Supporting Sciences Division through the award of grant HDTRA-08-1-0046 and Queen's University. In addition M.F.M. acknowledges the receipt of an NSERC Alexander Graham Bell post-graduate scholarship (CGS-D). The authors are grateful to Dr. Alexei A. Neverov of this department for useful discussions and also to Mr. Eric Keske of this department for assistance with elemental analysis.

Supporting Information Available: Tables of kinetic data and kinetic plots for the cleavage of **2** promoted by complexes **3,4,5,6,7,8,9**: $Zn(II)_2$ as a function of s_pH in methanol and $^1H/^{13}C$ NMR spectra for compounds **4** and **5**. This material is available free of charge via the Internet at <http://pubs.acs.org>.

(30) (a) Gibson, G.; Neverov, A. A.; Brown, R. S. *Can. J. Chem.* **2003**, *81*, 495. (b) For the designation of pH in non-aqueous solvents we use the nomenclature recommended by the IUPAC: *Compendium of Analytical Nomenclature. Definitive Rules 1997*, 3rd ed.; Blackwell: Oxford, U.K., 1998. The pH meter reading for an aqueous solution determined with an electrode calibrated with aqueous buffers is designated as s_wpH ; if the electrode is calibrated in water and the "pH" of the neat buffered methanol solution then measured, the term s_pH is used; and if the electrode is calibrated in the same solvent and the "pH" reading is made, then the term s_pH is used. In methanol $s_wpH - (-2.24) = s_pH$, and since the autoprotolysis constant of methanol is $10^{-16.77}$, neutral s_pH is 8.4.